



AIAA 2002-4246

Hall Thruster Modeling with a Given Temperature Profile

L. Dorf, V. Semenov *, Y. Raitses, N. J. Fisch
Princeton Plasma Physics Laboratory
Princeton, NJ

* Institute of Applied Physics of Russian Academy of Science
Nizhny Novgorod, Russia

**38th AIAA/ ASME/SAE/ASEE
Joint Propulsion Conference & Exhibit
7–10 July 2002
Indianapolis, Indiana**

For permission to copy or to republish, contact the copyright owner named on the first page.
For AIAA-held copyright, write to AIAA Permissions Department,
1801 Alexander Bell Drive, Suite 500, Reston, VA, 20191-4344.

HALL THRUSTER MODELING WITH A GIVEN TEMPERATURE PROFILE

L. Dorf, V. Semenov*, Y. Raitses and N.J. Fisch
Princeton Plasma Physics Laboratory (PPPL), Princeton, NJ 08543
** Institute of Applied Physics (IPFRAN), Nizhny Novgorod, Russia*

Abstract

A quasi one-dimensional steady-state model of the Hall thruster is presented. For given mass flow rate, magnetic field profile and discharge voltage the unique solution can be constructed, assuming that the thruster operates in one of the two regimes: with or without the anode sheath. It is shown that for a given temperature profile the applied discharge voltage uniquely determines the operating regime: for discharge voltages greater than a certain value, the sheath disappears. That result is obtained over a wide range of incoming neutral velocities, channel lengths and widths and cathode plane locations. A good correlation between the quasi 1-D model and experimental results can be achieved by selecting an appropriate temperature profile. We also show how the presented model can be used to obtain a two-dimensional potential distribution.

I. Introduction

Since the introduction of the main concept in the late 1950-s by Morozov¹ and Zharinov, various numerical models were proposed to describe physical processes in HT.²⁻⁹ To provide the existence and uniqueness of the solution in 1-D or quasi 1-D (considering wall losses) modeling with a given temperature profile one needs to introduce 3 boundary conditions. Since the applied discharge voltage is given, one needs to introduce 2 additional physical constraints on the free parameters.

Fruchtman and Fisch proposed in Ref. [10] that the requirement of sonic transition point, in which the ion velocity, V_i , equals to the sound velocity, V_s , to be regular can be used to determine one of the free parameters. To complete a model they assumed zero ion flow at the anode. Later Ahedo et al. in Ref. [2] assumed the presence of the back ion flow at the anode, $z=0$, and changed the condition $V_i(0) = 0$ to $V_i(0) = -V_s$, which appears to be more appropriate and results in a physically

valid solution over a wide range of discharge voltages. However, we show in this paper that for discharge voltages greater than a certain value this boundary condition also appears to be inappropriate.

In our model we introduce the boundary conditions, which result in the unique solution for all discharge voltages that are typically employed. For the same discharge voltage the Hall thruster may operate in one of the two regimes - with and without the anode sheath. If there is a sheath then, like in Ref [2], we obtain $V_i(0) = -V_s$. The electron velocity, V_e , in this case must be selected in order to obtain a total voltage drop in plasma equal to a given V_d . If there is no sheath then $V_e(0) = -V_{max}$, where V_{max} is determined only by the electron distribution function at the anode. A given V_d in this case determines the ion velocity. We resolve this indeterminacy numerically and show that for discharge voltages greater than a certain value anode sheath disappears. Thus, for a given temperature profile the applied discharge voltage uniquely determines the operating regime and therefore the type of the boundary conditions for V_{i0} and V_{e0} .

We make use of this approach to obtain the solution for the thruster channel and up to the cathode over a wide range of discharge voltages. We first use a simplified approach to certain issues namely, electron mobility and electron temperature profile, to focus the main attention on boundary conditions. But we also show how these issues can be resolved in order to construct a solution, which correlates well with experimental results for different mass flow rates and discharge voltages. To compare to experiment, we use the data obtained for the Princeton Plasma Physics Laboratory (PPPL) Hall thruster.¹² The calculated thruster performances namely, thrust, efficiency and propellant utilization, also appear to be in an agreement with experiment. Then we use a 1-D potential profile as a boundary condition on a channel median and solve a quasi 1-D problem in a radial direction to obtain a 2-D potential distribution.

This paper is organized as follows. In Sec. II we set up a physical problem and present a governing system of equations. In Sec. III we describe the boundary conditions indeterminacy and present a numerical procedure for determining the operating regimes and the free parameters. In Sec. IV we discuss numerically obtained solutions and present a new approach to determining a temperature profile using experimental data. In Sec. V we discuss “sheath” and “no sheath” regimes. We conclude in Sec. VI with obtaining a 2-D potential distribution.

II. Quasi 1-D model

Consider the conventional case of a HT with ceramic channel. The input parameters for any model of the HT are the experimentally controlled parameters, namely, the discharge voltage, V_d , the propellant mass flow rate, $\frac{dm}{dt}$, and the radial magnetic field profile, $B_r(z)$. We neglect the influence of the axial component of the magnetic field. The output parameters to be determined are the discharge current, I_d , the propellant utilization, and the profiles of ion velocity, ion density and potential.

To describe a steady-state operation of a Hall Thruster we consider the following physical processes. *Single ionization*: ions are born with the neutral velocity; *wall losses*: averaged over the channel cross-section; *ion acceleration*: toward the cathode, use hydrodynamic momentum equation for a mono-energetic ion flow with the ion velocity V_i ; *closed electron drift*: azimuthal, in $E_z \times B_r$ direction; *electron diffusion*: toward the anode, with the electron flow velocity V_e ; *free neutral motion*: assume the mono-energetic neutral flow with the constant neutral velocity V_{a0} . We also make a *quasineutrality* assumption: $n_i = n_e = n$, which is typical for a HT modeling.

In most of our numerical simulations we used input parameters typical for the PPPL Hall thruster operation:¹² $V_d = 150 - 300V$, $\frac{dm}{dt} = 1.7 - 3.0mg/s$ (propellant gas - Xenon), and $B_{max} \sim 130Gs$. We used the analytical fit consisting of six gauss-functions for magnetic field profile near the channel median as $B_r(z)$ (Fig. 1.)

In a 1-D description of a problem it is also necessary to select a distance from the anode, L_c , at

which the voltage drop equals to V_d , in other words make a choice of a cathode plane. We choose it to be the plane, where the cathode tip is physically located, $L_c = 5.4cm$ for the PPPL HT. This issue is discussed in a greater detail in Ref [22].

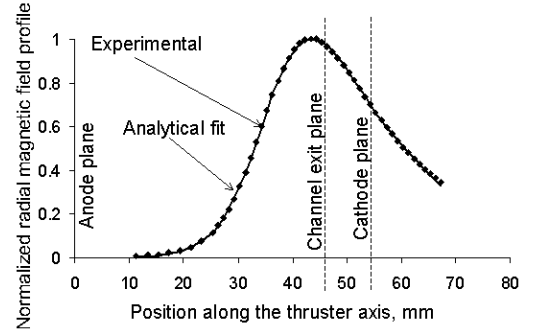


FIG. 1. Normalized magnetic field profile near the channel median for the PPPL HT

In our quasi 1-D model all vectors are projected on to the z - axis, where z is the coordinate along the thruster axis, with $z=0$ at the anode. The physical processes can be expressed mathematically as follows:

ION CONTINUITY EQUATION

$$(nV_i)' = \langle sV \rangle n_a n - \frac{2}{H_{ch}} \times 0.55 n \sqrt{\frac{T_e}{M_i}} \times \Theta(L_{ch} - z) \quad (1)$$

where the prime sign denotes the derivative with respect to z . In the first term of equation (1), the ionization constant, $\langle sV \rangle(T_e)$, was obtained using experimental data for ionization cross-section, $s_i^{Xe}(E_e)$.¹³ The electron distribution function was assumed to be Maxwellian with the local temperature T_e , and then the analytical approximation for $\langle sV \rangle(T_e)$ was deduced. In the second term H_{ch} and L_{ch} are the width and the length of a channel respectively ($H_{ch} = 1.8cm$, $L_{ch} = 4.6cm$ for PPPL HT); theta function, $\Theta(L_{ch} - z)$, represents the absence of the wall losses outside of the channel; and the factor of two indicates the presence of two channel walls. The factor of 0.55 was obtained by solving the radial sheath problem in the hydrodynamic description with the ionization and without collisions, as described by Reimann in Ref [14], however not assuming the quasineutrality in the presheath.

$$(nV_iV_i)' = \frac{eEn}{M_i} - \frac{2}{H_{ch}} \times 0.55n\sqrt{\frac{T_e}{M_i}} \times \Theta(L_{ch} - z) \times V_i + \langle \mathbf{S}V \rangle > n_a n V_{a0} \quad (2)$$

where E is the axial projection of the electric field and n_a is the neutral density.

CHARGE CONSERVATION

$$-nV_e + nV_i = J_d, \quad (3)$$

where $J_d = \frac{I_d}{eA_{ch}}$, e is electron charge, and $A_{ch} = 40.7\text{cm}^2$ is the channel cross-section.

ELECTRON MOMENTUM EQUATION

$$-en\mathbf{m}_e^{-1}V_e = eEn + (n_eT_e)', \quad (4)$$

We describe the electron axial motion with the phenomenological electron momentum equation, (4), in which \mathbf{m}_e is the absolute value of the electron axial mobility in a radial magnetic field.^{1,9} For the purposes of this paper it is sufficient to assume Bohm diffusion, i.e. $\mathbf{m}_e = \mathbf{m}_e^{Bohm} = \frac{1}{16B_r(z)}$.

However, in order for numerical simulations to be in an agreement with experiment, \mathbf{m}_e must be chosen more carefully, as we show later in this paper.

MASS CONSERVATION

$$n_a V_{a0} + nV_i = J_{a0} + J_{i0}, \quad (5)$$

where J_{a0} and J_{i0} are neutral and ion fluxes at the anode respectively. We consider that no ions are coming out of the anode, and all ions hitting the anode recombine with electrons and return to the discharge as neutrals. We therefore obtain:

$J_{a0} = J_m - J_{i0}$, where $J_m \stackrel{\text{def}}{=} \frac{dm/dt}{M_i A_{ch}}$ is the propellant flux. In simulations we consider a free molecular neutral flow out of the hot anode ($T_{anode} = 1000^\circ\text{C}$) to obtain $V_{a0} = 113\text{m/s}$.

$$T_e(z) = \text{Const} \quad (6)$$

Let us first consider a case of constant electron temperature. It is known from experiments, that $T_e \sim 3-5\text{eV}$ near the anode, and $T_e \sim 18-20\text{eV}$ in the maximum of the temperature profile,¹⁵ so we choose T_e from that interval in our numerical simulations. Later in this paper we return to the question of determining the temperature profile.

III. Boundary Conditions

The above system of equations can be reduced to the system of two ordinary differential equations for density, $n(z)$, and ion flux, $J_i(z) = n(z)V_i(z)$:

$$\left\{ \begin{array}{l} J_i' = n \langle \mathbf{S}V_e \rangle (T_e) \frac{J_m - J_i}{V_{a0}} - 1.1 \frac{n V_s}{H_{ch}} \\ n' = \frac{1}{1 - \frac{V_i^2}{V_s^2}} \left[\frac{e}{M_i \mathbf{m}_e V_s} \frac{J_d - J_i}{V_s} - \right. \\ \left. n \left((\ln T_e)' - \frac{\langle \mathbf{S}V_e \rangle (T_e)}{V_s} \frac{J_m - J_i}{V_s} \right) - \right. \\ \left. \frac{J_i}{V_s} \left(2 \frac{\langle \mathbf{S}V_e \rangle (T_e)}{V_s} \frac{J_m - J_i}{V_{a0}} - \frac{1.1}{H_{ch}} \right) \right], \end{array} \right. \quad (7)$$

where $V_s = \sqrt{\frac{T_e}{M_i}}$ is the ion acoustic velocity. The

Θ -function in terms originating from the wall-losses term in (1) was omitted for simplicity.

If the ion flux and the plasma density at the anode and the charge flux, J_d , are specified, one can try to integrate (7) numerically. In other words, the system (7) contains three free parameters to be determined before the solution can be obtained: n_0 ,

M_0 and \bar{V}_0 , where $M = \frac{V_i}{V_s}$, $\bar{V} = \frac{V_e}{V_{te}}$, $V_{te} = \sqrt{\frac{T_e}{m_e}}$ is

the electron thermal velocity, and the subscript ‘‘naught’’ means that functions are evaluated at the anode, $z = 0$. M_0 and \bar{V}_0 explicitly enter in the charge flux, $J_d = n_0(-\bar{V}_0 V_{te0} + M_0 V_{s0})$, and the ion flux at the anode, $J_{i0} = n_0 M_0 V_{s0}$. Thus, one needs three boundary conditions to provide the existence and uniqueness of the solution.

Neglecting wall losses in the ion continuity equation and assuming $V_{a0} = 0$ in the ion momentum equation, in order to better demonstrate our approach to determining the free parameters, we can deduce the following normalized equation for ion Mach number:

$$d_i M = \frac{(1+M^2)(1-J_i/J_m)\mathbf{b} - M^2(J_d/J_i - 1)\mathbf{g}}{1-M^2} \quad (8)$$

where $t \stackrel{\text{def}}{=} z/H_{ch}$, $\mathbf{b} \stackrel{\text{def}}{=} \frac{\langle sV \rangle (T_e) J_m H_{ch}}{V_{a0} V_s}$,

$\mathbf{g} \stackrel{\text{def}}{=} \frac{16w_{Bi} H_{ch}}{V_s}$, and $w_{Bi} = \frac{eB_r}{M_i}$ is the ion cyclotron frequency.

The equation (8) describes the ion dynamics in a quasineutral plasma. A similar equation describes the flow dynamics in the well-known de Laval nozzle.¹⁶ Other authors^{2,10} also dealt with this type of equation however, we find that there is still a need for additional analysis. The first (positive) term in the numerator of (8) originates from the ionization term in (1) and leads to ion acceleration in the subsonic region of the ion flow, i.e. where $M < 1$. The second (negative) term in the numerator of (8) is originally the electric field term from the equation (2), and it effectively works in subsonic plasma as an ion drag. The denominator appears essentially because of the electron pressure and it turns to zero at the boundary of the subsonic flow, at which $M=1$. This leads to a singularity, typical for quasineutral plasmas and called the ‘‘sonic transition’’.¹⁶ We look only for a non-singular solution of system (7) which describes a smooth behavior of all physical values in the vicinity of the sonic transition point, z_{st} , at which $M=1$. Fruchtman and Fisch in Ref. [10] considered the possibility of abrupt sonic transition in HT with an additional electrode placed inside the channel, and Ahedo *et al* in Ref. [2] proposed a ‘‘choked-exit’’ type of solution, in which ions reach the sound velocity right at the channel exit. However, all of the authors considered a smooth sonic transition in their models of the conventional Hall Thrusters.

As can be seen from (8), in order for the sonic transition point to be regular it is necessary that the drag and acceleration terms are equal at this point. Both of these terms depend on J_d and J_{i0} , i.e. on the free parameters that are set at $z=0$. Out of the three free parameters, only n_0 and M_0 enter explicitly in both J_d and J_{i0} , and, as will be shown

in the next paragraph, M_0 and \bar{V}_0 are physically interdependent. So, one can conclude that exactly the choice of n_0 is responsible for the smooth sonic transition. We set M_0 and \bar{V}_0 in the interval [0,1] and tried to select n_0 numerically in order to obtain a non-singular (NS) solution. It was shown by a comprehensive scanning over all reasonable for HT values of n_0 , that a smooth sonic transition takes place only if n_0 equals to a certain *unique* value, n_0^{NS} , which depends, of course, on (\bar{V}_0, M_0) . If $n_0 > n_0^{NS}$, the drag term appears to be too big and M does not reach 1 anywhere in the channel; and if $n_0 < n_0^{NS}$, the drag term is too small and a numerator in (8) appears to be greater than zero at z_{st} , which leads to a singularity (Fig. 2). Thus, for given (\bar{V}_0, M_0) the requirement of the sonic transition point to be regular results in the unique value of n_0 .

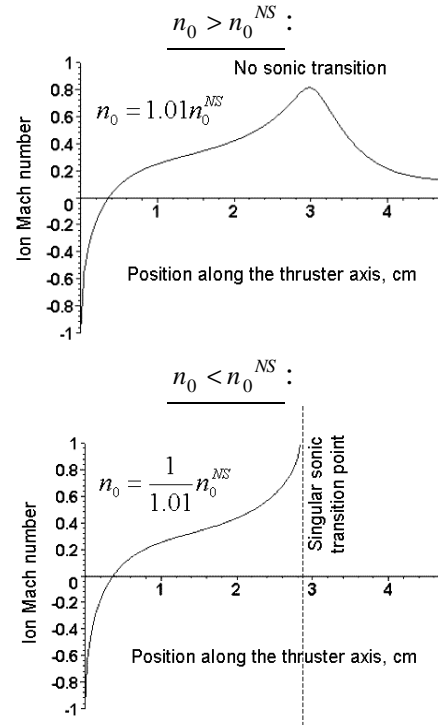


FIG. 1. Types of the ion velocity spatial behavior for different values of the plasma density at the anode. Case $T_e = Const$

There are two possibilities in determining \bar{V}_0 and M_0 . For the same discharge voltage the Hall thruster as every gas discharge may operate in one of the two regimes - with and without the anode sheath. If there is a sheath then, like in Ref [2], we obtain that $M_0 = -1$. The electron velocity, \bar{V}_0 , in

this case must be selected in order to obtain a total voltage drop in plasma equal to a given V_d :

$$\int_{0+}^{L_c} E(z) dz = V_d, \text{ where } L_c \text{ is the distance from the}$$

anode to the cathode plane, and “0+” means that the integration must be produced only over quasineutral plasma (we neglected a sheath voltage drop here, because T_e at the anode is usually very small in a real HT). If there is no sheath and plasma is quasineutral up to the anode, then $\bar{V}_0 = -\bar{V}_{\max}$, where \bar{V}_{\max} is determined only by the electron distribution function at the anode (we used $\bar{V}_{\max} = 0.4$ in our simulations, assuming Maxwellian distribution). In this case ions accelerated in the presheath toward the anode do not reach the sound velocity and M_0 is determined by a given V_d .

To resolve this indeterminacy we numerically scanned in the (\bar{V}_0, M_0) plane along the physically possible curve, as shown on Fig. 3. We found that V_d and I_d monotonically grow as we gradually transfer from “sheath” to “no sheath” regime. For $V_d > V_d^*$, where V_d^* corresponds to the point $(-\bar{V}_{\max}, -1)$ in the (\bar{V}_0, M_0) plane, there is no anode sheath. So, for given T_e and \mathbf{m} the discharge voltage, V_d , uniquely determines the operating regime and (\bar{V}_0, M_0) . The boundary condition issue is resolved.

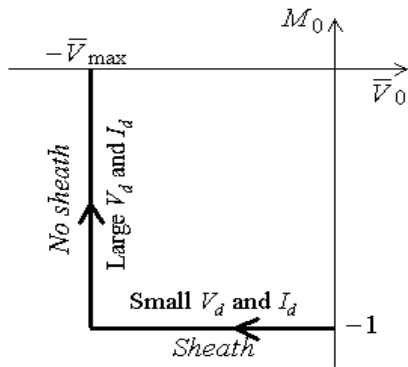


FIG.3. A physically possible curve in the (M_0, \bar{V}_0) cross-section of the free parameters space.

IV. Solution

The above boundary conditions were used to determine the free parameters and obtain solutions with several constant temperatures. It was found that, like in some other models,¹⁰ at large temperatures all of the propellant is ionized in a very short region near the anode, and at the smaller

temperatures the propellant utilization, $\frac{J_i(L_{ch})}{J_m}$,

appears to be atypically small for a HT. At temperatures smaller than a certain lower threshold, ionization appears to be insufficient for normal operation of the thruster and it becomes impossible to build a non-singular solution with supersonic ion velocity at the thruster exit with any free parameters.

It was shown that the same approach to determining the free parameters can be applied in the case of any given shape of temperature profile, qualitatively similar to experimental,¹⁵ if maximal temperature, T_{\max} , is chosen to be large enough (see Appendix). We investigated the dependence of the solution on the shape of the temperature profile, and for each considered point $[V_d, J_m, B_r(z)]$ in the typical PPPL HT operational range were able to determine $T_e(z)$ that results in the experimental

value of I_d and $\frac{n_{\max}}{n_0} \sim 10$, which is typical for

HT.¹⁵ From the same argument we have determined the actual value of electron mobility: $\mathbf{m}_e \sim (1/8 - 1/6)\mathbf{m}_e^{Bohm}$. The fact that electron mobility in Hall thrusters appears to be several times less than the one obtained with a Bohm diffusion concept was also discovered by some other authors.^{8,17,18}

The numerically obtained profiles for $V_d = 240V$ and a mass flow rate of 1.7 mg/s are shown on Fig. 4. It was found that $M_0 = -1$ and $\bar{V}_0 = -0.06$ for such input parameters, so the thruster operates in a “sheath” regime. The propellant utilization (about 86%) and potential utilization profile were found to be in an agreement with experiment.^{12,19} We have also calculated the thruster performances namely, thrust, T , and efficiency, \mathbf{h} , using the following expressions:

$$T = S_{ch} J_i(L_c) M_i V_i(L_c), \quad \mathbf{h} = \frac{T^2}{2 \frac{dm}{dt} I_d V_d}.$$

The results also turned out to be in a correlation with experiment: $T = 25mN$, $\mathbf{h} = 47\%$.¹²

V. Discussions

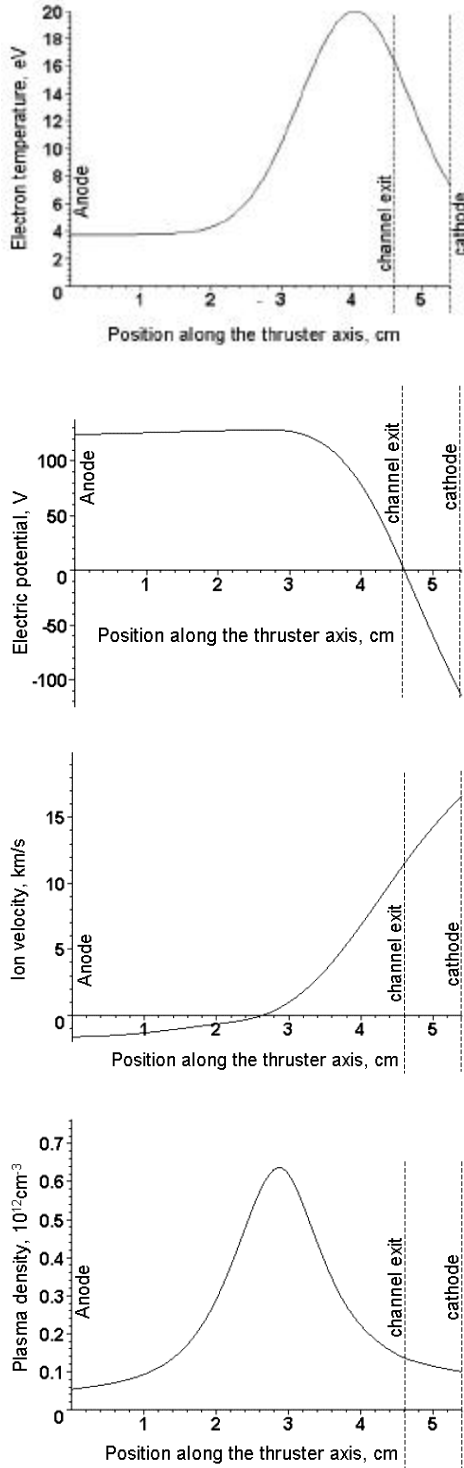


FIG. 4 The numerically obtained profiles in a Hall thruster.

$$\text{For } V_d = 240 \text{ V}, \quad \frac{dm}{dt} = 1.7 \text{ mg/s}.$$

Zero potential was chosen at the channel exit.

$$z_{st} = 3.52 \text{ cm}, \quad I_d = 1.63 \text{ A}$$

The temperature profile found for $V_d = 240\text{V}$ and $\frac{dm}{dt} = 1.7\text{mg/s}$ was used to obtain solutions for $\frac{dm}{dt} = 1.7\text{mg/s}$ at several discharge voltages and the same $B_r(z)$. The numerically obtained thruster $V-I$ characteristic is presented on the Fig. 5. The $V-I$ characteristics with corresponding $T_e(z)$ were also obtained for the mass flow rates of 2mg/s and 2.5mg/s , and for several channel lengths and widths. For most of the considered (V_d, J_m) in the typical PPPL HT operational range the anode sheath appeared to take place. So, at moderate discharge voltages $M_0 = -1$ can be used as a universal BC for modeling of a HT, as suggested in Ref. 2. As was shown, \bar{V}_0 in this case must be selected in order to obtain a desired V_d . The negative ion flux toward the anode was indeed measured in experiments.¹⁵ But for discharge voltages greater than a certain value, V_d^* , which increases when the mass flow rate is increased, sheath disappeared and in order to obtain a solution it was necessary to use alternative, “no sheath” type boundary conditions: $\bar{V}_0 = -\bar{V}_{\max}$, M_0 is determined by V_d . The “no sheath” regime was also observed experimentally²⁰. It was found that for the same V_d , J_m and $B_r(z)$ an absolute value of \bar{V}_0 increases and may even reach \bar{V}_{\max} when the channel length from the anode side is artificially decreased. It was also discovered that V_d^* , separating “sheath and “no sheath” regimes, increases when the electron mobility is increased.

The presented quasi 1-D model with a given temperature profile is, of course, simplified and not completely suitable for a quantitative description of the real thruster behavior in the experiments. However, it proved to be useful for a qualitative analysis and for better understanding of the HT operation in a wide range of input parameters. The main results are recognizing a possibility of the thruster operation without the anode sheath and presenting a method of determining the thruster operating regime and the free parameters for a 1-D modeling. The presented approach involves only global physical phenomena: anode sheath and sonic transition. So, it can be suggested that this approach is applicable for a 2-D modeling, especially considering that 2-D effects take place mainly in the region of a strong magnetic field, far from the anode. Let us also notice that the applicability of the

described approach to determining the free parameters was shown for different profiles of the magnetic field, qualitatively similar to the one used in a PPPL HT. The authors also believe that the same approach can be applied for modeling of other types of Hall thrusters such as *segmented electrode HT* and *anode layer thruster*.^{12, 21}

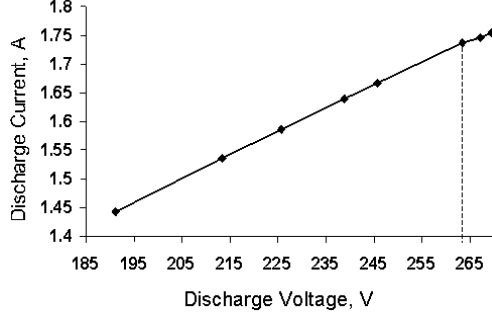


FIG. 5. The numerically obtained Hall thruster V-I characteristic. $\frac{dm}{dt} = 1.7 \text{ mg/s}$. For $V_d > 263 \text{ V}$ there is no anode sheath.

VI. 2-D Potential distribution

A quasi 1-D model can be used to obtain an approximate 2-D potential distribution. Let us consider a planar geometry with z -axis along the channel median and r -axis in the radial direction. The ion continuity equation and the radial projection of the ion momentum equation then become:

$$\frac{\partial J_z}{\partial z} + \frac{\partial J_r}{\partial r} = \langle \mathbf{S}V \rangle n_a n_e \quad (9)$$

where J_z and J_r are the axial and the radial projections of the ion flux respectively. We assume for simplicity that $\frac{\partial J_r}{\partial r}$ is independent of r and that $J_r(z, 0) = 0$, i.e. that ion flux on the channel median is purely axial. Then $\frac{\partial J_r}{\partial r} = \frac{\Gamma_{wall}}{H_{ch}/2}$, where Γ_{wall} is ion flux to the wall. As was already mentioned, it can be shown that $\Gamma_{wall} = 0.55 n(z, 0) \sqrt{\frac{T_e(z)}{M_i}}$; electron temperature is assumed independent of r .

Thus, we obtain:

$$\frac{\partial J_r}{\partial r} = 1.1 \frac{n(z)}{H_{ch}} \sqrt{\frac{T_e(z)}{M_i}}, \quad (10)$$

where $n(z)$ is a plasma density obtained from a quasi 1-D modeling. We assume all the quantities on a channel median to be those found from a quasi 1-D modeling.

Let us introduce the following normalized variables: $t = r/r_d$, $u = e(\mathbf{j} - \mathbf{j}(z))/T_e(z)$, $e = \partial u / \partial t$, $N_{e,i} = n_{e,i} / n(z)$, where $r_d = \sqrt{T_e(z) / 4pn(z)e^2}$, \mathbf{j} is electric potential, $\mathbf{j}(z)$ is electric potential obtained from a quasi 1-D modeling, and $n_{e,i}$ are the electron and ion densities (we give up a quasineutrality assumption away from the channel median). We assume a Boltzman distribution for electrons:

$$N_e = \exp(u) \quad (11)$$

A quasineutrality assumption made in a 1-D modeling leads to the following form of a Poisson equation:

$$\partial e / \partial t = N_e - N_i \quad (12)$$

Using a radial projection of the ion momentum equation: $\frac{\partial(V_z J_r)}{\partial z} + \frac{\partial(V_r J_r)}{\partial r} = e E_r n_i / M_i$, together with equations (10) – (12) and neglecting $\frac{\partial(V_z J_r)}{\partial z}$ for simplicity, we can deduce the following approximate expression for the normalized ion density:

$$N_i = \frac{(I t)^2}{e^2 / 2 + 1 - \exp(u)}, \quad (13)$$

where $I = 1.1 r_d(z) / H_{ch}$.

The equations (11) – (13) can be independently integrated along r in every point on a z -axis with a local value of $r_d(z)$. Since $u(0) = 0$ by definition of u , we only need to supply the above system with one more boundary condition on a channel median: $e(z, 0) = 0$. The numerically obtained 2-D potential distribution is presented on a Fig. 6. The shape of the equipotentials is found to be in a reasonable agreement with experiment.¹⁹

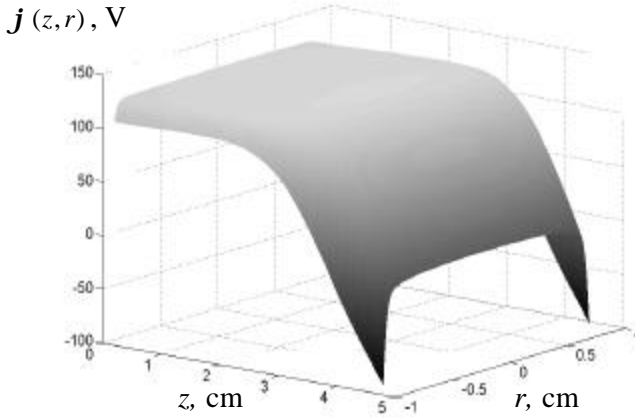


FIG. 6. Numerically obtained 2-D potential distribution. For $V_d = 240 V$, $\frac{dm}{dt} = 1.7 mg/s$.

Appendix: Selection of the appropriate T_{max}

As was mentioned, in order for the described approach to determining free parameters to work properly for discharge voltages in the practically used range, T_{max} for the electron temperature profile, $T_e(z) = T_{max} \cdot \text{Shap}\epsilon(z)$, must be chosen large enough for a given m . Otherwise, as we move in the (\bar{V}_0, M_0) plane along the physically possible curve from “Sheath” to “No sheath” region (Fig. 3), we will find the discharge current to very slowly increase, whereas the discharge voltage will significantly decrease. Of course, in the real HT the decrease of discharge voltage at the same magnetic field profile leads to the decrease of a discharge current and, as was shown before, the decrease of V_d should occur when we move from “No sheath “to” Sheath region, not on the contrary. It was shown that at the same mass flow rate the minimal value of T_{max} depends strongly on the incoming neutral velocity. Basically, if T_{max} for which solution can be constructed with a certain V_{a0} is known, then in order to be able to construct a solution with another V_{a0} , T_{max} must be chosen so that to keep $\frac{\langle sV \rangle (T_{max})}{V_{a0}}$ approximately the same.

Acknowledgement

The authors would like to thank M. Keidar, D. Staack, A. Smirnov and A. Litvak for very useful discussions and their comments on this paper.

This work was partially supported by the US DOE under contract No. DE-AC02-76CH03073 and the Russian Foundation for Basic Research.

References

1. A. I. Morozov and V. V Savelyev, in the “Reviews of Plasma physics”, edited by B. B. Kadomtsev and V. D. Shafranov, vol. 21
2. E. Ahedo, P. Martinez-Cerezo, M. Martinez-Sanches, Phys. Plasmas 8, 3058 (2001)
3. E. Ahedo, P. Martinez-Cerezo, M. Martinez-Sanches, AIAA paper No. 2001-3323, 37-th Joint Propulsion Conference and Exhibit, July 8-11 2001, Salt Lake City, Utah
4. I. Katz, G. Jongeward, V. Davis, M. Mandell, I. Mikellides, R. Dressler, I. Boyd, K. Kannenberg, AIAA paper No. 2001-3355, 37-th Joint Propulsion Conference and Exhibit, July 8-11 2001, Salt Lake City, Utah
5. I. G. Melikidze, I. Katz, M. Mandell, J. S. Snyder, AIAA paper No. 2001-3505, 37-th Joint Propulsion Conference and Exhibit, July 8-11 2001, Salt Lake City, Utah
6. M. Keidar, I. D. Boyd, J. Appl. Phys. 86, 4786 (1999)
7. D. B. VanGilder, I. D. Boyd, M. Keidar, J. Spacecraft Rockets 37, 129 (2000)
8. M. Keidar, I. D. Boyd, and I. I. Beilis, Phys. Plasmas 8, 5315 (2001)
9. K. Makowsky, Z. Peradzynski, N. Gascon, and M. Dudeck, AIAA paper No. 1999-2295, 35-th Joint Propulsion Conference and Exhibit, June 20-24 1999, Los Angeles, California
10. A. Fruchtman, N. J. Fisch and Y. Raitses, Phys. Plasmas 8, 1048 (2001)
11. V. I. Baranov, Y. S. Nazarenko, V. A. Petrosov, A. I. Vasin, IEPC paper No. 99-103, 26-th International Electric Propulsion Conference, Oct. 17-21, 1999, Kokura-kita, Kitakyushu, Japan
12. Y. Raitses, L. A. Dorf, A. A. Litvak, and N. J. Fisch, J. Appl. Phys. 88, 1263 (2000)
13. D. Rapp and P. Englander-Golden, J. Chem. Phys. 43, 1464 (1965)
14. K-U Riemann, J. Phys. D: Appl. Phys. 24, 493 (1991)
15. A. M. Bishaev and V. Kim, Sov. Phys. Tech. Phys. 23, 1055 (1978)
16. F. I. Frank, Izvestia Akademii Nauk SSSR, Ser. Matematika, vol. IX, 1945
17. E. Ahedo, P. Martinez, and M. Martinez-Sanches, AIAA paper No. 2000-3655, 36-th Joint Propulsion Conference, Huntsville, AL
18. J. M. Fife and S. Locke, AIAA paper No. 2001-1137, 39-th Aerospace Sciences Meeting and Exhibit, Reno, NV, Jan. 8-11, 2001
19. Y. Raitses, M. Keidar, D. Staack and N. J. Fisch, J. Appl. Phys., submitted Nov. 2001
20. A. I. Bugrova and V. Kim, in “Plasma Accelerators and Ion Injectors” (Nauka, Moscow, 1984) 107 (in Russian)
21. V. V. Zhurin, H. R. Kaufman and R. S. Robinson, Plasma Sources Sci. Technol., 8, R1-R20 (1999) (printed in the UK)
22. L. Dorf, V. Semenov, Y. Raitses, N.J. Fisch, submitted to Phys. Plasmas, Mar, 2002